

November 15, 1991

Magnetic-properties and local ordering during thermal annealing of amorphous $\text{Fe}_{75}\text{Ni}_5\text{B}_{15}\text{Si}_5$ films

S. A. Oliver

V. G. Harris
Northeastern University

C. Vittoria
Northeastern University

W. T. Elam

K. H. Kim

See next page for additional authors

Recommended Citation

Oliver, S. A.; Harris, V. G.; Vittoria, C.; Elam, W. T.; Kim, K. H.; Hamdeh, H. H.; and Alhabash, M., "Magnetic-properties and local ordering during thermal annealing of amorphous $\text{Fe}_{75}\text{Ni}_5\text{B}_{15}\text{Si}_5$ films" (1991). *Electrical and Computer Engineering Faculty Publications*. Paper 75. <http://hdl.handle.net/2047/d20002246>

Author(s)

S. A. Oliver, V. G. Harris, C. Vittoria, W. T. Elam, K. H. Kim, H. H. Hamdeh, and M. Alhabash



Magnetic properties and local ordering during thermal annealing of amorphous Fe₇₅Ni₅B₁₅Si₅ films

S. A. Oliver, V. G. Harris, C. Vittoria, W. T. Elam, K. H. Kim et al.

Citation: *J. Appl. Phys.* **70**, 5852 (1991); doi: 10.1063/1.350134

View online: <http://dx.doi.org/10.1063/1.350134>

View Table of Contents: <http://jap.aip.org/resource/1/JAPIAU/v70/i10>

Published by the [American Institute of Physics](http://www.aip.org).

Related Articles

Finite-size scaling relation of the Curie temperature in barium hexaferrite platelets

J. Appl. Phys. **110**, 123909 (2011)

Enhanced refrigerant capacity and magnetic entropy flattening using a two-amorphous FeZrB(Cu) composite

Appl. Phys. Lett. **99**, 232501 (2011)

Nonlinear motion of magnetic vortex under alternating-current magnetic field: Dynamic correction of a gyrovecton and a damping tensor of the Thiele's equation

Appl. Phys. Lett. **99**, 142505 (2011)

High domain wall magneto-resistance in amorphous TbFeCo wires

Appl. Phys. Lett. **99**, 122501 (2011)

Accurate measurement of domain wall velocity in amorphous microwires, submicron wires, and nanowires

Rev. Sci. Instrum. **82**, 094701 (2011)

Additional information on *J. Appl. Phys.*

Journal Homepage: <http://jap.aip.org/>

Journal Information: http://jap.aip.org/about/about_the_journal

Top downloads: http://jap.aip.org/features/most_downloaded

Information for Authors: <http://jap.aip.org/authors>

ADVERTISEMENT

LakeShore Model 8404 developed with
NEW AC/DC Hall Effect System  **TOYO Corporation**
Measure mobilities down to 0.001 cm²/V s

Magnetic properties and local ordering during thermal annealing of amorphous $\text{Fe}_{75}\text{Ni}_5\text{B}_{15}\text{Si}_5$ films

S. A. Oliver

Center for Electromagnetics Research, Northeastern University, Boston, Massachusetts 02115

V. G. Harris^{a)} and C. Vittoria

Department of Electrical and Computer Engineering, Northeastern University, Boston, Massachusetts 02115

W. T. Elam and K. H. Kim^{b)}

Code 4683, U.S. Naval Research Laboratory, Washington, DC 20375

H. H. Hamdeh and M. Alhabash

Department of Physics, Wichita State University, Wichita, Kansas 67208

The evolution of magnetic properties and local atomic ordering during thermal annealing has been studied for amorphous $\text{Fe}_{75}\text{Ni}_5\text{B}_{15}\text{Si}_5$ thin films. Resistivity, vibrating sample magnetometer (VSM), ferromagnetic resonance (FMR), extended x-ray absorption fine structure (EXAFS), and Mössbauer effect (ME) measurements were taken on samples annealed at various temperatures ranging to film crystallization. The as-deposited samples are in a close-packed structure with little short-range order. Samples annealed above 200 °C show ordering of the boron shell, but no indication of long-range ordering. With the exception of the anisotropy and coercive fields, no change in the magnetic or microwave magnetic parameters is observed for these samples prior to crystallization. Samples annealed above 400 °C show indications of crystallization for all measurements.

Amorphous magnetic alloys generally require post-deposition processing to develop desirable soft magnetic properties. This often entails usage of thermal treatments. However, it is unclear how the changes in the local atomic environment produced by thermal annealing affect the macroscopic magnetic properties. Such knowledge can be obtained by combining probes of the local atomic environment with measurements of the sample magnetic properties. Here such results are presented for an iron-rich Fe-Ni-B-Si alloy. The advantages of this alloy with respect to earlier Co-Fe-B-Si alloys studied include a higher crystallization temperature and better soft magnetic properties.¹ This alloy is also amenable to Mössbauer effect measurements, which provide information on the local chemical environment.

A film was deposited onto a polished fused quartz wafer by ion-beam sputtering from a 99% pure pressed powder $\text{Fe}_{75}\text{Ni}_5\text{B}_{15}\text{Si}_5$ target. Base chamber pressure before deposition was 3.8×10^{-8} Torr, with the pressure during film deposition maintained at 1.3×10^{-4} -Torr purified argon. Maximum temperature reached by the film during deposition was ~ 50 °C. Film thickness was found to be 148 nm by surface profilometer. Magnetic and structural measurements on a dozen 5-mm-diam samples cored from this film constitute the data set for this study.

Samples were thermally annealed in flowing argon gas oven mounted in the gap of a vibrating-sample magnetometer (VSM). Annealing conditions were as follows: the sample was placed with the hard axis aligned along the

magnetic field; then annealed at fixed temperature for a 16-min period in a 500-Oe applied magnetic field; a hysteresis loop was performed; finally the film was cooled without an applied field. Ferromagnetic resonance (FMR) measurements were taken using a 9.5-GHz resonant cavity, with the applied magnetic field aligned either in the film plane (parallel) or normal to the film plane (perpendicular).

Local ordering in the films was deduced from the results of room-temperature extended x-ray absorption fine structure (EXAFS) and Mössbauer effect (ME) measurements. EXAFS measurements were taken on beam-line X-23B at the National Synchrotron Light Source at Brookhaven National Laboratory. Details of the beam-line characteristics, electron yield EXAFS technique, and data analysis have been presented elsewhere.^{1,2} Conversion electron Mössbauer effect spectra were obtained on four samples using a 50-mCi ⁵⁷Co radiation source in a rhodium matrix. Due to the small sample sizes involved ME spectra were collected over a 350-h period, assuring that over two million counts were available for each sample.

Fourier transforms calculated from iron *K*-edge EXAFS data for the as-deposited and annealed samples are displayed in Fig. 1. Superimposed at the top of Fig. 1 is the Fourier transform of a polycrystalline bcc-Fe film. Since the displayed radial coordinates are uncorrected for an electron phase shift only qualitative comparisons can be made between the amorphous samples and the bcc-Fe standard. Examination of Fig. 1 indicates that the appearance of long-range order in the Fourier transform occurs only for samples annealed at or above 400 °C, where the distinct signature of bcc local symmetry appears for the sample annealed at 475 °C.

^{a)}Current address: U.S. Naval Research Laboratory, Code 4683, Washington DC 20375-5000.

^{b)}Supported by the NRC fellowship program.

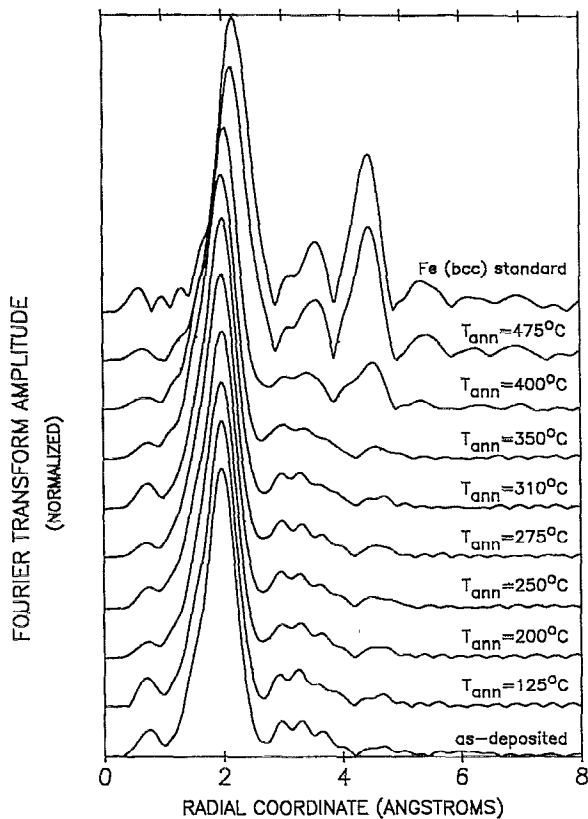


FIG. 1. Superposition of Fourier transforms of iron EXAFS spectra taken on annealed samples, with radial coordinates uncorrected for electron phase shift. At the top for comparison is a spectrum taken on a polycrystalline bcc-Fe sample. Peaks appearing near 1 Å are artifacts of the data analysis.

Quantitative modeling of EXAFS data was used in extracting the coordination number, radial distances, and Debye-Waller factors of the nearest-neighbor shells to the iron atoms.³ First shell EXAFS fitting of as-deposited sample data are best modeled by a single shell of boron atoms at a radial distance of 2.11 ± 0.02 Å (coordination number = 2.25 ± 0.25 B atoms), surrounded by a pair of iron atom shells, the inner shell at a radial distance of 2.48 ± 0.02 Å (coord. no. = 3.5 ± 0.5 Fe atoms), the outer shell at 2.68 ± 0.02 Å (coord. no. = 7.0 ± 2.0 Fe atoms). These fitting parameters remain approximately constant for samples annealed below 175 °C. The boron shell Debye-Waller factor decreases from the as-deposited value for samples annealed above 175 °C, having a minima at 200 °C, and then slowly increasing for samples annealed at higher temperatures. No other changes are apparent for samples annealed at temperatures lower than 400 °C. Fits for both samples annealed above 400 °C show evolving changes in the iron shells: the coordination number of the inner Fe shell increases to 5.8 ± 0.5 Fe atoms along with a significant decrease in the Debye-Waller factor, while the radial distance remains constant; the radial distance of the second Fe shell expands in progression from 2.68 to 2.71 Å to 2.84 ± 0.2 Å. Changes are also observed in the boron shell fit parameters for these samples: the coordination number increases to 3.5 ± 0.5 B atoms, while the Debye-Waller factor increases

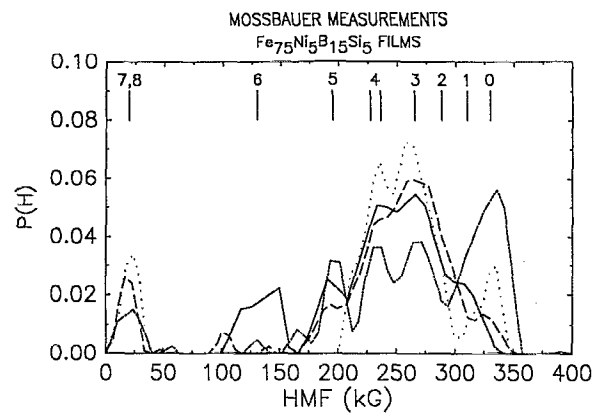


FIG. 2. Probability distribution of the hyperfine magnetic fields for the as-deposited (—), 200 (---), 310 (···), and 475 °C (-·-·-) annealed samples.

by almost a factor of 3 over the as-deposited fit value.

Mössbauer effect measurements provide information on the chemical short-range order. Figure 2 shows the calculated ^{57}Fe hyperfine magnetic field (HMF) distributions generated using the method of Le Caër and Dubois.⁴ Numbered vertical hash marks are included in Fig. 2 at positions which approximate HMF values found for iron borides, with the labels being the number of boron atom nearest neighbors (nn). These values include α -Fe (0 B nn) and the iron borides FeB (6 B nn), Fe_2B (4 B nn),⁵ and tetragonal t - Fe_3B (2, 3, and 4 B nn sites).⁶ Orthorhombic o - Fe_3B has two iron sites, both with 3 B nn, but with differing HMF fields such that one site corresponds to 4 B nn in Fig. 2.⁷ Fe sites having 1 or 5 B nn do not occur for typical ordered Fe-B phases, and will thus be considered indicators of an amorphous local environment. The HMF for Fe atoms having 5 B nn was deduced from Vincze *et al.*,⁸ while the HMF corresponding to 1 B nn was deduced using the assumption that 2 B nn perturb the HMF twice as much as 1 B nn for dilute alloys. HMF values for paramagnetic Fe atoms having 7 or 8 B nn are also displayed. Values for the average hyperfine magnetic field (HMF) are given in Table I.

Sample saturation magnetization remained constant within experimental accuracy, with an average value of $4\pi M_s = 15.3 \pm 03$ kG. The resistivity of the annealed samples remained roughly constant at $\rho = 139 \pm 4$ $\mu\Omega$ cm, decreasing to $\rho = 96$ $\mu\Omega$ cm for the sample annealed at 475 °C. An abrupt change in coercive field values measured at elevated temperatures occurs for samples annealed at, and above 225 °C, dropping from the as-deposited values to under 0.01 Oe. The room-temperature normalized coercive field (taking into account variations between samples) systematically decreases for samples annealed at higher temperatures, until a dramatic increase is seen at 400 °C. This trend is similar to that reported on cobalt-rich films.¹

Sample in-plane (H_k) and perpendicular anisotropy fields (H_u^{\perp}) were obtained from FMR measurements. The in-plane anisotropy is seen to decrease relative to the as-deposited sample average of $H_k = 15 \pm 3$ Oe for all sam-

TABLE I. The annealing temperature (T_{ann}), in-plane anisotropy field, effective magnetization, average hyperfine magnetic field (HMF), and exchange stiffness constant are listed for all samples.

T_{ann} (°C)	H_k (Oe)	$4\pi M_{\text{eff}}$ (kG)	HMF (kG)	A ($\times 10^{-6}$ erg/cm)
AD	18.7	15.35	237	0.89
125	10.9	15.41	...	0.96
175	13.0	15.58	...	0.98
200	3.1	15.62	234	0.98
225	6.2	15.71	...	0.96
250	6.8	15.88	...	0.97
275	4.7	15.41	...	0.95
310	5.2	15.84	235	1.01
350	5.7	16.14	...	0.96
400	3.6	16.14	...	0.95
475	257	...

ples annealed above 200 °C (see Table I). A slight increase in H_u^1 with increased annealing temperature is indicated from the effective magnetization values ($4\pi M_{\text{eff}} = 4\pi M_s + H_u^1$), also displayed in Table I. Calculated values for the Landé g factor were virtually constant at $g = 2.085 \pm 0.001$ for all annealed samples measured. Well defined spin-wave resonance (SWR) spectra were obtained from perpendicular FMR measurements for all samples. Higher order SWR modes obeyed the quadratic dispersion relation, and were used in deducing the exchange stiffness constant (A) listed in Table I. Extraneous modes were observed for the sample annealed at 400 °C. These modes occur at much higher magnetic fields than the FMR main line, and are attributed to formation of small crystallized regions in the sample. FMR main-line linewidths were consistently near 55 Oe for all samples.

The combination of EXAFS and ME results show that the average iron atom in the as-deposited film has a close-packed structure with little short-range order. The HMF distribution indicates that Fe sites having from 1–6 B nn have sizable probabilities of being present, including Fe sites having 1 or 5 B nn which do not conform to typical Fe-B intermetallics. HMF distributions for samples annealed at 200 and 310 °C show a diminishing probability of finding Fe sites having 1, 5, and 6 B nn, while the probability of a Fe site corresponding to α -Fe or paramagnetic Fe increases. The behavior of the boron Debye-Waller factor, in combination with the HMF distributions, imply that the nearest-neighbor boron shell orders near 200 °C, with ordering of iron in an α -Fe environment occurring at a higher temperature, shown by the growth of the 0 B nn peak between the sample annealed at 200 and 310 °C in Fig. 2. The disruption of boron atoms caused by preferential ordering of many Fe sites in an α -Fe local environment causes the boron Debye-Waller factor to rise. The preva-

lence of Fe sites having HMF near 3 or 4 B nn is consistent with earlier studies, which have shown formation of metastable Fe_3B phases in related alloys.^{9,10}

Changes in the magnetic properties for samples annealed below 400 °C are observed only for the anisotropy and coercive fields. The drop in H_k from as-deposited values occurs for the same sample that has the smallest boron Debye-Waller fitting factor. This suggests that ordering of the boron shell may be important for internal stress relief. The remaining measured properties are seen to be insensitive to the changes in local environment inferred from the EXAFS and ME results.

Beginning with the sample annealed at 400 °C, nearly all measurements show indications of long-range ordering. Considerable reorganization of both iron shells is apparent in EXAFS, with both EXAFS and ME results indicating that a considerable fraction of Fe atoms are in the bcc α -Fe phase. This was confirmed by rotating anode x-ray diffraction measurements, which show distinct α -Fe diffraction peaks. ME line shapes indicate that Fe sites having HMF values attributable to Fe_3B environments are also common. However, these samples have not fully crystallized, since the sample still possesses a large fraction of iron sites having local environments that do not correspond to either α -Fe or the iron-boride phases, indicated by the substantial ME peaks corresponding to 1 or 5 B nn in Fig. 2. These results are consistent with previous annealing studies on bulk quenched samples,⁹ although, in general, crystallization products for these thin-film samples are observed at lower temperatures than for the bulk samples.

We gratefully acknowledge B. Fultz for x-ray diffraction measurements; P. Dorsey, J. P. Kirkland, and B. Katz for assistance with EXAFS data collection and beam-line operation; and National Science Foundation Young Scholars N. Darling, C. Kowalewski, and S. Miller for assistance with the static magnetization data. This research was carried out in part at the National Synchrotron Light Source, which is sponsored by the U. S. Department of Energy.

¹V. G. Harris, S. A. Oliver, W. B. Nowak, C. Vittoria, K. H. Kim, and W. T. Elam, *J. Appl. Phys.* **69**, 5457 (1991).

²R. A. Neiser, J. P. Kirkland, W. T. Elam, and S. Sampath, *Nucl. Instrum. Methods A* **266**, 220 (1988).

³J. J. Rehr, J. Mustre de Leon, and S. I. Zabinski, *J. Am. Chem. Soc.* (to be published).

⁴G. Le Caër and J. M. Dubois, *J. Phys. E* **12**, 1083 (1979).

⁵L. Takács, M. C. Cadeville, and I. Vincze, *J. Phys. F* **5**, 800 (1975).

⁶G. Le Caër and J. M. Dubois, *Phys. Status Solidi A* **64**, 275 (1981).

⁷W. K. Choo and R. Kaplow, *Metall. Trans. A* **8**, 417 (1977).

⁸I. Vincze, D. S. Boudreaux, and M. Tegze, *Phys. Rev. B* **19**, 4896 (1979).

⁹M. Takahashi, M. Koshimura, and T. Abuzuka, *Jpn. J. Appl. Phys.* **20**, 1821 (1981).

¹⁰F. H. Sanchez, Y. D. Zhang, J. I. Budnick, and R. Hasegawa, *J. Appl. Phys.* **66**, 1671 (1989).